In Vivo Expression of Reprogramming Factor OCT4 Ameliorates Myelination Deficits and Induces Striatal Neuroprotection in Huntington's Disease

Ji Hea Yu
Yonsei University College of Medicine
Bae-Geun Nam
Yonsei University College of Medicine
MinGi Kim
Yonsei University College of Medicine
Jung Hwa Seo
Yonsei University College of Medicine
Sung-Rae Cho (srcho918@yuhs.ac)
Yonsei University College of Medicine https://orcid.org/0000-0003-1429-2684

Research

Keywords: Huntington's disease, reprogramming, octamer-binding transcription factor 4, oligodendrocyte progenitor cells

Posted Date: June 18th, 2020

DOI: https://doi.org/10.21203/rs.3.rs-33786/v1

Version of Record: A version of this preprint was published at Genes on May 10th, 2021. See the published version at https://doi.org/10.3390/genes12050712.

Abstract

Background: White matter atrophy has been shown to precede the massive loss of striatal GABAergic neurons in Huntington's disease (HD). The HD-induced white matter atrophy is associated with motor deficits. *In vivo* reprogramming toward a plastic state has emerged as a new approach for treating neurological diseases. Particularly, octamer-binding transcription factor 4 (OCT4) can induce myelin repair and functional recovery. This study investigated the effects of *in situ* expression of reprogramming factor OCT4 on behavioral performances, neural stem cell (NSC) niche activation in the subventricular zone (SVZ) and induction of cell fate specific to the changed microenvironment of HD.

Methods: R6/2 mice, a transgenic mouse model of HD, randomly received adeno-associated virus serotype 9 (AAV9)-OCT4, AAV9-Null, or phosphate-buffered saline in both lateral ventricles at 4 weeks of age**.** To evaluate the behavioral improvement, rotarod test and grip strength test were performed at regular intervals. To investigate the expression of oligodendrocyte progenitor cell (OPC)-related genes, real-time quantitative reverse transcription PCR (qRT-PCR) and immunohistochemistry were performed. Next, we assessed the amelioration of myelination deficits via transmission electron microscope (TEM) and magnetic resonance imaging (MRI) at 13 weeks of age. Finally, we confimed striatal neuroprotecion by qRT-PCR and confocal microscopy.

Results: The AAV9-OCT4 group displayed significantly improved rotarod performance and grip strength compared to the control groups. Following AAV9-OCT4 treatment, the number of newly generated NSCs and OPCs was significantly increased in the SVZ, and the expression of OPC-related genes such as NG2, Olig2, PDGFRα, Wnt3 and myelin regulatory factor (MYRF), and glial cell-derived neuroprotective factor (GDNF) was significantly increased. Further, the amelioration of myelination deficits in the corpus callosum was observed through TEM and MRI, and striatal $DARPP32^{+}$ GABAergic neurons significantly increased in the AAV9-OCT4 group.

Background

Huntington's disease (HD) pathology is characterized by massive loss of neurons in striatum and deep layers of the cortex as well as early and progressive thinning of white matter (WM) in the corpus callosum [1]. Although the mechanism underlying abnormalities of WM has not been confirmed, neuroimaging data supports the hypothesis that myelin breakdown leads to WM atrophy in human and mouse models of HD [2, 3]. Recent studies have shown that WM atrophy precedes striatal atrophy [4, 5] and causes motor and emotional defects in HD [6, 7].

Under demyelinating conditions, neural stem cells (NSCs) and neural progenitors proliferate, migrate, and give rise to oligodendrocyte progenitor cells (OPCs), and then differentiate into myelinating oligodendrocytes. However, chronic diseases with extensive myelin loss can limit remyelination [8, 9]. *In vivo* reprogramming toward a plastic state has emerged as a new approach for treating neurological diseases [10, 11]. Previous studies revealed that the ectopic expression of OCT4, a key reprograming

factor, is sufficient to directly reprogram NSCs into a pluripotent and plastic state [12–14]. Myelin repair and functional recovery can be enhanced by the application of lentiviral OCT4 and OCT4-induced OPCs in animal models of demyelinated optic chiasm [10] and spinal cord injury [10], respectively.

This study investigated the effects of *in vivo* expression of OCT4 on NSC niche activation in the subventricular zone (SVZ) and induction of cell fate specific to the changed microenvironment of HD. Finally, we found that the *in situ* expression of OCT4 in the SVZ induces OPC proliferation, thereby attenuating myelination deficits. Additionally, myelin regulatory factor (MYRF) and glial cell-derived neuroprotective factor (GDNF) released by OPCs induced striatal neuroprotection in HD, which can explain the behavioral improvement in R6/2 mice overexpressing OCT4.

Materials And Methods

Mice

R6/2 strain, a transgenic mouse model of HD carrying approximately 160 ± 5 CAG repeats, was obtained from the Jackson Laboratory (B6CBA-Tg (HDexon1) 62Gpb/1J, Stock No: 002810). These transgenic mice mimic human HD with many neurological phenotypes, including choreiform-like movements, involuntary stereotypic movements, tremor, epileptic seizures, and non-movement disorder components including unusual vocalization. The symptoms of R6/2 mice become apparent between 6 and 8 weeks of age. All animals were housed in a facility accredited by the Association for Assessment and Accreditation of Laboratory Animal Care (AAALAC). Experimental procedures were approved by the Institutional Animal Care and Use Committee (IACUC 2016 – 0298).

Stereotaxic injection

At 4 weeks of age, mice were anesthetized with intraperitoneal (IP) injection of ketamine (100 mg/kg; Huons, Gyeonggi-do, Korea) and xylazine (10 mg/kg; Bayer Korea, Seoul, Korea). A stereotaxic procedure was performed at 4 weeks of age in which the mice received a lateral ventricular (LV) injection (1×10^{12} vg/ml, 1 µl each) using the following stereotaxic coordinates: AP + 0.3 mm from bregma, ML ± 0.7 mm from bregma, and DV − 2.0 mm from dura mater (Fig. 1A). Adeno-associated virus serotype 9 (AAV9) vector (ViroVek, Hayward, CA, USA) containing human OCT4 was expressed using the cytomegalovirus (CMV) promotor (AAV9-OCT4). Mice were randomly assigned to one of the following groups: phosphate-buffered saline (PBS), AAV9-Null, or AAV9-OCT4 treatment.

Behavioral analyses

Rotarod test

A rotarod test (No.47600, Ugo Basile, Comerio, Italy) was used to assess motor coordination and locomotor function at 4, 6, 8, 10, and 13 weeks of age. The rolling rod was set to an accelerating speed (4

~ 40 rpm) and a constant speed (16 rpm), and the latency fall time was measured [15]. An individual test was terminated at a maximum latency of 300 seconds if the mouse did not fall.

Grip strength test

A grip strength test was performed using the SDI Grip Strength System (San Diego Instruments, Inc., San Diego, CA, USA), which includes a push-pull strain gauge at 4, 8 and 12 weeks of age. A 2-mm diameter triangular piece of metal wire was used as the grip bar. Each animal was held near the base of its tail by a researcher and allowed to approach the bar until it was able to grip it with its forepaw. Peak grip force was automatically recorded in kilogram-force (kgf) by the apparatus. The average of peak forces from the three trials was used for the final analysis [15]. Grip force data from the grip strength test were normalized with respect to body weight [16].

Immunohistochemistry (IHC)

Mice were daily given an IP injection of BrdU (50 mg/kg, Sigma-Aldrich, St. Louis, MO) for 12 days, beginning after stereotaxic surgery [11]. R6/2 mice at 6 weeks and 13 weeks of age were sacrificed by transcardial perfusion with cold PBS, followed by 4% paraformaldehyde (PFA). Harvested brain tissues were cryosectioned 16-mm thick slices, and immunohistochemical staining was performed on four sections, representing a range of more than 128 μm. The tissue sections were stained with the following antibodies: 5-bromo-2'-deoxyuridine (BrdU, 1:200, abcam, ab6326); neuron-specific class III beta-tubulin (βIII-tubulin, 1:400, abcam, ab18207); glial fibrillary acidic protein (GFAP, 1:400, abcam, ab10062); Nestin (1:400, abcam, ab6142); neural/glial antigen 2 (NG2, 1:200, Millipore, ab5320) and dopamine- and cAMP-regulated neuronal phosphoprotein (DARPP-32, 1:400, cell signaling technology, 2306). The stained sections were analyzed using confocal microscopy (LSM700, Zeiss, Gottingen, Germany).

Real-time quantitative reverse transcription PCR (qRT-PCR)

At 13 weeks of age, R6/2 mice were sacrificed for biochemical study and perfused with cold PBS. Total RNA was extracted from the cortex and the striatum using TRIzol (Invitrogen Life Technologies, Carlsbad, CA, USA). Purified total RNA (1 μg) was used as a template to generate the cDNA using the ReverTra Ace qPCR RT master mix with gDNA remover (TOYOBO). The standard protocol for the qRT-PCR with SYBR Green was provided from roche applied science. A total volume of 20 μl master mix with 1 μl of cDNA was used in the qRT-PCR reaction, which was performed in triplicate on a LightCycler 480 using the LightCycler 480 SYBR Green master mix (Roche Applied Science, Mannheim, Germany). The mRNA abundance of target genes was assayed by qRT-PCR. Glyceraldehyde 3-phosphate dehydrogenase was used as an internal control. The expression of each gene of interest was obtained using the $2^{-\Delta\Delta Ct}$ method.

Transmission electron microscopy (TEM)

For TEM study, mice were perfused and fixed for 12 hours in 0.1M phosphate buffer (PB) followed by 4% PFA containing 2% glutaraldehyde (MERCK, ZC814139734) at 13 weeks of age. They were postfixed with

1% osmium tetroxide dissolved in 0.1M PB for 2 hours and dehydrated inascending gradual series (50 ~ 100%) of ethanol and infiltrated with propylene oxide. Specimens were embedded by Poly/Bed 812 kit (Polysciences). After pure fresh resin embedding and polymerization at 65 °C electron microscope oven (TD-700, DOSAKA, Japan) for 24 hours. Sections of about 200 ~ 250 nm thick section were initially cut and stained with toluidine blue (sigma, T3260) for light microscope. Ultra-thin slices (70 nm) were double stained with 6% uranyl acetate (EMS, 22400 for 20 min) and lead citrate (fisher, for 10 min) for contrast staining. There sections were cut by LEICA EM UC-7 (Leica Microsystems, Austria) with a diamond knife (Diatome) and transferred on copper and nickel grids. All of the thin sections were observed by transmission electron microscopy (JEM-1011, JEOL, Japan) at the acceleration voltage of 80 kV. For image analyses, axon and myelin fiber diameters were measured using Image J (NIH).

Magnetic resonance imaging (MRI)

At 13 weeks of age, R6/2 mice were anaesthetised with 1 ~ 3% isoflurane. MRI experiments were performed with a 9.4 T Bruker Biospec scanner (Ettlingen, Germany) running Paravision 5.1, using a 40 mm transreceive coil. Following the acquisition of the anatomical images using the rapid acquisition with the relaxation enhancement (RARE) protocol, diffusion experiments were conducted using the DTI echo planar imaging (DTI-EPI) protocol. The imaging parameters were: slice thickness 0.32 mm, 20 slices, matrix size of 128 × 128 with 0.156 mm x 0.156 mm resolution, δ/Δ = 4/10 ms, 30 directions with b = 670 s/mm^2 and TE/TR = 23.5/5000 ms. Diffusion images were processed using DSI studio software (http://dsi-studio.labsolver.org). The processed data were further analyzed with MATLAB (MathWorks, Natick MA) to obtain fractional anisotropy (FA), radial diffusivity (RD) and axial diffusivity (AD).

Statistical analysis

The results are presented as mean ± SEM were determined variables compared among groups by one-way ANOVA with post-hoc multiple comparisons using SPSS statistics version 23.0 (IBM Corporation, Armonk, NY, USA). Statistical significance was considered when $P < 0.05$.

Results

In vivo **expression of OCT4 improves behavioral performance**

An initial evaluation was performed before the stereotaxic injection using rotarod and grip strength tests. Following the treatment, mice were evaluated using identical measures until terminal stage (12 ~ 13 weeks of age). The AAV9-OCT4 group showed a significant increase in latency compared to the control groups in the accelerating speed rotarod test (4 ~ 40 rpm) at 13 weeks of age (PBS = 10 ± 2.2, AAV9-Null = 7.1 ± 1.2, AAV9-OCT4 = 40.6 ± 13.4 s) (Fig. 1B) and in the constant speed rotarod test (16 rpm) at 10 weeks (PBS = 16 ± 2.9, AAV9-Null = 30 ± 7.6, AAV9-OCT4 = 138.1 ± 65.8 s) and 13 weeks of age (PBS = 10.7 ± 3.7, AAV9-Null = 8.3 ± 2.7, AAV9-OCT4 = 34.7 ± 20.5 s) (Fig. 1C). The AAV9-OCT4 group also displayed significantly increased grip force compared to the control groups and in the grip strength test at 8 weeks (PBS = 4.4 ± 0.6, AAV9-Null = 4.5 ± 0.3, AAV9-OCT4 = 6.1 ± 0.2 g) and 12 weeks of age (PBS = 4.3

± 0.2, AAV9-Null = 4.1 ± 0.3, AAV9-OCT4 = 5.9 ± 0.4 g) (Fig. 1D). These results suggest that OCT4 plays a primary role in improving behavioral performance in HD mice.

In situ **expression of OCT4 increases NSCs and OPCs in the SVZ**

BrdU can track newly proliferated cells via IHC analysis. Therefore, we evaluated the fate of NSCs or neurons in the SVZ by counting the numbers of cells expressing $Nestin^{+}BrdU^{+}$ or $\beta III\text{-}tubulin^{+}BrdU^{+}$. Newly proliferated cells that could possibly differentiate into OPCs or astrocytes were evaluated by counting the numbers of $NG2^{+}BrdU^{+}$ or $GFAP^{+}BrdU^{+}$ expressing cells. Two weeks after treatment, the fate of NSCs in the SVZ at 6 weeks of age was evaluated through IHC. In the SVZ, the numbers of $Nestin^{+}BrdU^{+}$ (PBS = 1.17 ± 0.4, AAV9-Null = 1.4 ± 0.4, AAV9-OCT4 = 5.7 ± 1.7 ($x10^3$ cells/mm^3)) and $NG2^{+}BrdU^{+}$ (PBS = 2.4 ± 1.5, AAV9-Null = 2.2 ± 0.3, AAV9-OCT4 = 4.6 ± 1.1 ($x10^3$ cells/mm^3)) cells were significantly higher in the AAV9-OCT4 group than the controls (Fig. 2A, B). The numbers of $\beta III\text{-}tubulin^{+}BrdU^{+}$ (PBS = 2.3 ± 1.0, AAV9-Null = 2.0 ± 0.7, AAV9-OCT4 = 2.7 ± 1.7 ($x10^3$ cells/mm^3)) and $GFAP^{+}BrdU^{+}$ (PBS = 1.7 ± 0.8, AAV9-Null = 1.7 ± 0.8, AAV9-OCT4 = 4.4 ± 1.1 ($x10^3$ cells/mm^3)) cells did not significantly differ among the three groups (Fig. 2C, D). These findings demonstrated that *in situ* expression of OCT4 in the SVZ increases the number of newly generated NSCs and OPCs but not the number of newly generated neurons and astrocytes in HD mice. We hypothesize that the *in situ* expression of OCT4 can induce the NSC proliferation in the SVZ, which in turn can converge into more number of OPCs within the microenvironmental clues of HD.

Oct4-induced Opcs Ameliorate Myelination Deficits Of Hd Mice

Next, we confirmed the effects of OCT4 on OPC-related gene expression specific to the microenvironment in HD. Expression of OPC-related markers NG2, oligodendrocyte transcription factor 2 (Olig2), platelet-derived growth factor receptor alpha (PDGFRα), Wnt family member 3 (Wnt3), myelin regulatory factor (MYRF), and GDNF was confirmed by qRT-PCR at 13 weeks of age. The AAV9-OCT4 group displayed significantly increased expression levels of OPC-related markers in the cortex (Fig. 3A) and striatum (Fig. 3B).

TEM and MRI were used to visualize myelinated fibers in corpus callosum (CC) at 13 weeks of age. In the CC, the g-ratio of the AAV9-OCT4 group was significantly lower than the controls (Fig. 4A). When MRI results were analyzed for FA, RD and AD, myelination defects were significantly reduced in the AAV9-OCT4 group (Fig. 4B). These results suggested that OCT4 overexpression induces myelin plasticity via the activation of OPC-related genes and ameliorates myelination deficits of HD mice.

Subependymal Oct4 Expression Induces Striatal Neuroprotection

Expression of markers neuronal nuclei (NeuN), glutamic acid decarboxylase 65 (GAD65) and GFAP was confirmed by qRT-PCR at 13 weeks of age. AAV9-OCT4 group displayed significantly increased expression of NeuN, a mature neuronal marker in the cortex and GAD65, a GABAergic neuronal marker in the striatum. However, the AAV9-OCT4 group did not change the expression of GFAP, an astrocytic marker in both regions (Fig. 5A). In the striatum, the area of DARPP-32$^+$ GABAergic neurons significantly increased in the AAV9-OCT4 group compared to control groups using confocal microscopy (Fig. 5B). OPCs have been shown to express various growth factors and cytokines that play a significant role in cell functions and survival [17, 18]. Previous studies reported that GDNF, mainly released by OPCs and oligodendrocytes, can promote neuronal cell survival as well as axon regeneration and myelination in demyelinating conditions [17, 19]. Taken together, these results raise the potential that OCT4 overexpression not only ameliorates myelination deficits but also induces striatal neuroprotection in HD.

Discussion

Recent studies have reported that WM is associated with motor and cognitive functions, which explains why HD-induced WM atrophy causes the behavioral defects [6, 7]. The pre-symptomatic (pre-HD) stage of R6/2 mice shows myelin deficits in the corpus callosum at 4 weeks of age before the remarkable GABAergic neuronal loss, which is known to occur at late-symptomatic (late-HD) stage. In this study, following *in vivo* expression of reprogramming factor OCT4 in pre-HD R6/2 mice, the rotarod and grip strength tests revealed significant motor improvements in the late-HD stage of OCT4-overexpressing mice compared to the control groups, suggesting that OCT4 may be the primary role in improving behavioral performance in HD mice (Fig. 1B-D).

We then observed that OCT4 using AAV9 vector administrated into the LV have effect on the NSC niche activation in the SVZ. The SVZ contains the largest niche areas for newly generated neural cells such as neurons and glial cells in the adult brain [20–23]. In the damaged WM areas, therapeutic mechanism to induce endogenous NSC activation in the SVZ can change the fate of NSCs into oligodendrocyte-lineage cells in order to compensate for myelin deficits [23]. Namely, *in situ* expression of OCT4 in the SVZ increased the number of newly generated NSCs (Nestin$^+$BrdU$^+$ cells) and OPCs (NG2$^+$BrdU$^+$ cells) but not the number of newly generated neurons (βIII-tubulin$^+$BrdU$^+$ cells) and astrocytes (GFAP$^+$BrdU$^+$ cells) in HD mice (Fig. 2A-D). This result demonstrated that the microenvironmental clues of HD specifically induce the cell fate from NSCs to OPCs in the SVZ.

Next, we confirmed the effects of OCT4 on OPC-related gene expression specific to the microenvironment in HD. The OCT4-induced OPCs enhanced myelin plasticity via the activation of OPC-related genes (Fig. 3A, B). NG2 and Olig2 are used to specifically identify OPCs [24]. Olig2, PDGFRa and Wnt3 induce the differentiation of OPCs to oligodendrocytes [25–27]. Particularly, our results displayed that OCT4-induced OPCs upregulated MYRF expression. Since HD causes MYRF downregulation and leads to oligodendrocyte death and demyelination [28], OCT4-mediated MYRF upregulation can ameliorate myelination deficits in the WM of brains with HD. In addition, OPCs have been shown to express various growth factors and cytokines that play a significant role in cell functions and survival [17, 18]. Previous

studies reported that GDNF, mainly released by OPCs and oligodendrocytes, can promote neuronal cell survival as well as axon regeneration and myelination in demyelinating conditions [17, 19]. The neuroprotective functions of secreted GDNF also could benefit GABAergic neurons in the striatum and mitigate the effects of HD, all of which have been reported to improve behavioral functions.

For the analysis of health axon with myelin in CC via analysis of TEM images, g-ratio was calculated in each axon with myelin. The values of g-ratio of AAV9-OCT4 group were significantly lower than those in control groups, indicating that OCT4 overexpression ameliorated myelination deficits of HD mice (Fig. 4A). It is important to note that FA is positively correlated to the myelination and organization of WM fibers [29], and early increase in RD and AD are followed by significant changes in neuronal volume loss in HD [30–32]. Our data showed that AAV9-OCT4 group had significantly higher FA and lower RD, AD compared to control groups (Fig. 4B). Our biochemical results demonstrated that OCT4 overexpression also protected mature neurons, not astrocytes, in the cortex and striatum (Fig. 5A). Particularly, expression of striatal DARPP32^{+} GABAergic neurons significantly increased in the AAV9-OCT4 group compared to control groups (Fig. 5B).

Conclusion

In situ expression of reprogramming factor OCT4 induces NSC niche activation in the SVZ and changes cell fate specific to the microenvironment of HD from NSCs to OPCs. Particularly, MYRF and GDNF released by OPCs seem to ameliorate myelination deficits and induce striatal neuroprotection in HD, which explains the behavioral improvement such as motor coordination and grip strength in R6/2 mice overexpressing OCT4 (Fig. 6). Taken together, these results raise the potential that OCT4-induced OPCs not only ameliorates myelination deficits but also induces striatal neuroprotection in HD.

Abbreviations

HD
Huntington’s disease; WM:white matter; CC:corpus callosum; NSCs:neural stem cells; OPCs:oligodendrocyte progenitor cells; OCT4:octamer-binding transcription factor 4; SVZ:subventricular zone; PBS:phosphate-buffered saline, AAV9:adeno-associated virus serotype 9; CMV:cytomegalovirus, vg:viral genomes; LV:lateral ventricle; AP:anteroposterior; ML:mediolateral; DV, dorsoventral; qRT-PCR:quantitative reverse transcription polymerase chain reaction; TEM:transmission electron microscope; MRI:magnetic resonance imaging; FA:fractional anisotropy; RD:radial diffusivity; AD:axial diffusivity; PFA:paraformaldehyde, IP:ntraperitoneal; BrdU:5-bromo-2'-deoxyuridine; NG2:neural/glial antigen 2; Olig2:oligodendrocyte transcription factor; PDGFRα:platelet-derived growth factor receptor alpha; Wnt3:Wnt family member 3; MYRF:myelin regulatory factor; GDNF:glial cell-derived neuroprotective factor; βIII-tubulin:neuron-specific class III beta-tubulin; NeuN:neuronal nuclei; GAD65:glutamic acid decarboxylase 65; DARPP32:dopamine- and cAMP-regulated neuronal phosphoprotein

Declarations

Acknowledgments

We thank Medical Illustration & Design, part of the Medical Research Support Services of Yonsei University College of Medicine for all artistic supports related to this work, Eun Jin Kim, part of the electron microscopy of Yonsei Biomedical Research Center, and Dr. Chan Gyu Joo, Severance Biomedical Science Institute of Yonsei University College of Medicine, for technical supports, and Soonil Pyo for proofreading the manuscript.

Authors' contributions

JHY and B-GN equally contributed to this study. JHY performed most of the experiments, analyzed data, and wrote the manuscript; B-GN performed most of molecular study, analyzed data, and wrote the manuscript; MGK performed experiments, and wrote manuscript; JWS performed animal experiments; S-RC developed the study concept and design, wrote the maunscript, and supervised the project. All authors read and confirmed the maunscript.

Funding

This research was supported by Basic Science Research Program through the National Research Foundation of Korea (NRF) funded by the Ministry of Education (grant number : 2019R1I1A1A01057970) and the Korean Health Technology R&D Project through the Korea Health Industry Development Institute (KHIDI), funded by the Ministry of Health & Welfare, Republic of Korea (grant number : HI16C1012)

Availability of data and materials

All relevant data that support the findings of this study are available from the corresponding author upon reasonable request.

Ethics approval

All animals were housed in a facility accredited by the Association for Assessment and Accreditation of Laboratory Animal Care (AAALAC). Experimental procedures were approved by the Institutional Animal Care and Use Committee (IACUC 2016-0298).

Consent for publication

Not applicable.

Competing interests

We declare that we do not have any commercial or associative interest that represents a conflict of interest in connection with the work submitted.

Author details

[1]Department and Research Institute of Rehabilitation Medicine, Yonsei University College of Medicine, Republic of Korea

[2]Brain Korea 21 PLUS Project for Medical Science, Yonsei University, Republic of Korea

[3]Graduate Program of Nano Science and Technology, Yonsei University, Republic of Korea

References

1. Ross CA, Aylward EH, Wild EJ, Langbehn DR, Long JD, Warner JH, et al. Huntington disease: natural history, biomarkers and prospects for therapeutics. Nat Rev Neurol. 2014;10(4):204–16.
2. Gatto RG, Ye AQ, Colon-Perez L, Mareci TH, Lysakowski A, Price SD, et al. Detection of axonal degeneration in a mouse model of Huntington's disease: comparison between diffusion tensor imaging and anomalous diffusion metrics. Magma. 2019;32(4):461–71.
3. Gregory S, Cole JH, Farmer RE, Rees EM, Roos RA, Sprengelmeyer R, et al. Longitudinal Diffusion Tensor Imaging Shows Progressive Changes in White Matter in Huntington's Disease. J Huntingtons Dis. 2015;4(4):333–46.
4. Jin J, Peng Q, Hou Z, Jiang M, Wang X, Langseth AJ, et al. Early white matter abnormalities, progressive brain pathology and motor deficits in a novel knock-in mouse model of Huntington's disease. Hum Mol Genet. 2015;24(9):2508–27.
5. Teo RT, Hong X, Yu-Taeger L, Huang Y, Tan LJ, Xie Y, et al. Structural and molecular myelination deficits occur prior to neuronal loss in the YAC128 and BACHD models of Huntington disease. Hum Mol Genet. 2016;25(13):2621–32.
6. Beglinger LJ, Nopoulos PC, Jorge RE, Langbehn DR, Mikos AE, Moser DJ, et al. White matter volume and cognitive dysfunction in early Huntington's disease. Cogn Behav Neurol. 2005;18(2):102–7.
7. Faria AV, Ratnanather JT, Tward DJ, Lee DS, van den Noort F, Wu D, et al. Linking white matter and deep gray matter alterations in premanifest Huntington disease. Neuroimage Clin. 2016;11:450–60.
8. Franklin RJ. Why does remyelination fail in multiple sclerosis? Nat Rev Neurosci. 2002;3(9):705–14.
9. Imitola J, Snyder EY, Khoury SJ. Genetic programs and responses of neural stem/progenitor cells during demyelination: potential insights into repair mechanisms in multiple sclerosis. Physiol Genomics. 2003;14(3):171–97.
10. Dehghan S, Hesaraki M, Soleimani M, Mirnajafi-Zadeh J, Fathollahi Y, Javan M. Oct4 transcription factor in conjunction with valproic acid accelerates myelin repair in demyelinated optic chiasm in mice. Neuroscience. 2016;318:178–89.
11. Seo JH, Lee MY, Yu JH, Kim MS, Song M, Seo CH, et al. In Situ Pluripotency Factor Expression Promotes Functional Recovery From Cerebral Ischemia. Mol Ther. 2016;24(9):1538–49.
12. Kim JB, Zaehres H, Arauzo-Bravo MJ, Scholer HR. Generation of induced pluripotent stem cells from neural stem cells. Nat Protoc. 2009;4(10):1464–70.

13. Kim JB, Sebastiano V, Wu G, Arauzo-Bravo MJ, Sasse P, Gentile L, et al. Oct4-induced pluripotency in adult neural stem cells. Cell. 2009;136(3):411–9.
14. Kim JB, Greber B, Arauzo-Bravo MJ, Meyer J, Park KI, Zaehres H, et al. Direct reprogramming of human neural stem cells by OCT4. Nature. 2009;461(7264):649–3.
15. Cho SR, Suh H, Yu JH, Kim HH, Seo JH, Seo CH. Astroglial Activation by an Enriched Environment after Transplantation of Mesenchymal Stem Cells Enhances Angiogenesis after Hypoxic-Ischemic Brain Injury. Int J Mol Sci. 2016;17(9).
16. Ge X, Cho A, Ciol MA, Pettan-Brewer C, Snyder J, Rabinovitch P, et al. Grip strength is potentially an early indicator of age-related decline in mice. Pathobiol Aging Age Relat Dis. 2016;6:32981.
17. Wilkins A, Majed H, Layfield R, Compston A, Chandran S. Oligodendrocytes promote neuronal survival and axonal length by distinct intracellular mechanisms: a novel role for oligodendrocyte-derived glial cell line-derived neurotrophic factor. J Neurosci. 2003;23(12):4967–74.
18. Ettle B, Schlachetzki JCM, Winkler J. Oligodendroglia and Myelin in Neurodegenerative Diseases: More Than Just Bystanders? Mol Neurobiol. 2016;53(5):3046–62.
19. Gao X, Deng L, Wang Y, Yin L, Yang C, Du J, et al. GDNF Enhances Therapeutic Efficiency of Neural Stem Cells-Based Therapy in Chronic Experimental Allergic Encephalomyelitis in Rat. Stem Cells Int. 2016;2016:1431349.
20. Gonzalez-Perez O, Alvarez-Buylla A. Oligodendrogenesis in the subventricular zone and the role of epidermal growth factor. Brain Res Rev. 2011;67(1–2):147–56.
21. Ihrie RA, Alvarez-Buylla A. Lake-front property: a unique germinal niche by the lateral ventricles of the adult brain. Neuron. 2011;70(4):674–86.
22. Falcão AM, Marques F, Novais A, Sousa N, Palha JA, Sousa JC. The path from the choroid plexus to the subventricular zone: go with the flow! Front Cell Neurosci. 2012;6:34.
23. Maki T, Liang AC, Miyamoto N, Lo EH, Arai K. Mechanisms of oligodendrocyte regeneration from ventricular-subventricular zone-derived progenitor cells in white matter diseases. Front Cell Neurosci. 2013;7:275.
24. El Waly B, Macchi M, Cayre M, Durbec P. Oligodendrogenesis in the normal and pathological central nervous system. Front Neurosci. 2014;8:145.
25. Lu QR, Sun T, Zhu Z, Ma N, Garcia M, Stiles CD, et al. Common developmental requirement for Olig function indicates a motor neuron/oligodendrocyte connection. Cell. 2002;109(1):75–86.
26. Lo Nigro A, de Jaime-Soguero A, Khoueiry R, Cho DS, Ferlazzo GM, Perini I, et al. PDGFRα(+) Cells in Embryonic Stem Cell Cultures Represent the In Vitro Equivalent of the Pre-implantation Primitive Endoderm Precursors. Stem Cell Reports. 2017;8(2):318–33.
27. Zawadzka M, Rivers LE, Fancy SP, Zhao C, Tripathi R, Jamen F, et al. CNS-resident glial progenitor/stem cells produce Schwann cells as well as oligodendrocytes during repair of CNS demyelination. Cell Stem Cell. 2010;6(6):578–90.

28. Huang B, Wei W, Wang G, Gaertig MA, Feng Y, Wang W, et al. Mutant huntingtin downregulates myelin regulatory factor-mediated myelin gene expression and affects mature oligodendrocytes. Neuron. 2015;85(6):1212–26.
29. Pierpaoli C, Barnett A, Pajevic S, Chen R, Penix LR, Virta A, et al. Water diffusion changes in Wallerian degeneration and their dependence on white matter architecture. Neuroimage. 2001;13(6 Pt 1):1174–85.
30. Rosas HD, Lee SY, Bender AC, Zaleta AK, Vangel M, Yu P, et al. Altered white matter microstructure in the corpus callosum in Huntington's disease: implications for cortical "disconnection". Neuroimage. 2010;49(4):2995–3004.
31. Bohanna I, Georgiou-Karistianis N, Sritharan A, Asadi H, Johnston L, Churchyard A, et al. Diffusion tensor imaging in Huntington's disease reveals distinct patterns of white matter degeneration associated with motor and cognitive deficits. Brain Imaging Behav. 2011;5(3):171–80.
32. Delmaire C, Dumas EM, Sharman MA, van den Bogaard SJ, Valabregue R, Jauffret C, et al. The structural correlates of functional deficits in early huntington's disease. Hum Brain Mapp. 2013;34(9):2141–53.

Figures

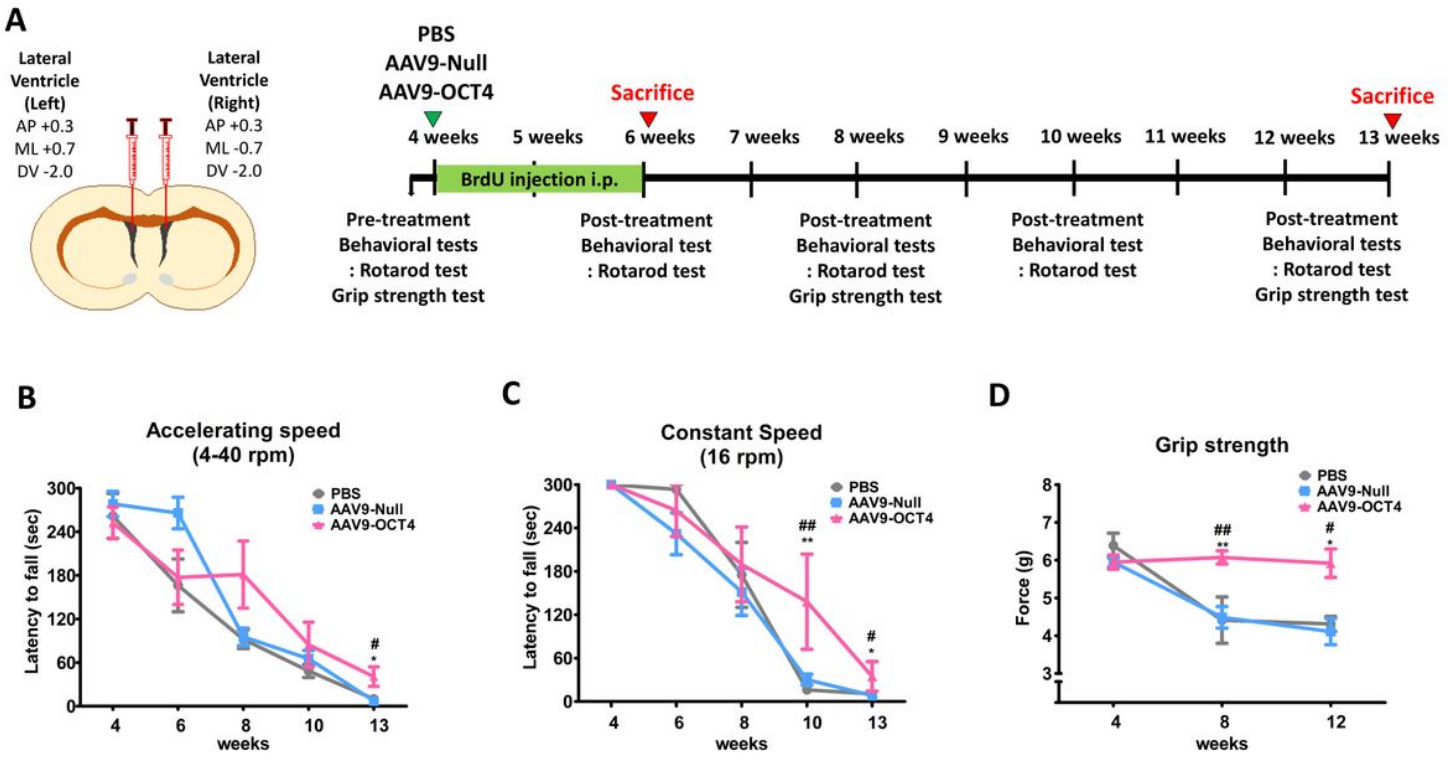

Figure 1

In vivo expression of OCT4 improves behavioral performance in Huntington's disease mice. (A) Stereotaxic surgery and the schedule of behavioral tests in the timeline are presented. (B-D) AAV9-OCT4

group displayed significant improvements compared to the control groups (AAV9-Null and PBS) at week 13 in the accelerating rotarod test (4–40 rpm) (B), at weeks 10 and 13 in the constant rotatrod test (16 rpm) (C) and at weeks 8 and 12 in the grip strength test (D). #,*p<0.05, ##,**p<0.01, Data in all panels represent mean ± SEM. *PBS vs AAV9-OCT4, #AAV9-Null vs AAV9-OCT4. OCT4: octamer-binding transcription factor 4, AAV9: adeno-associated virus serotype 9, PBS: phosphate-buffered saline

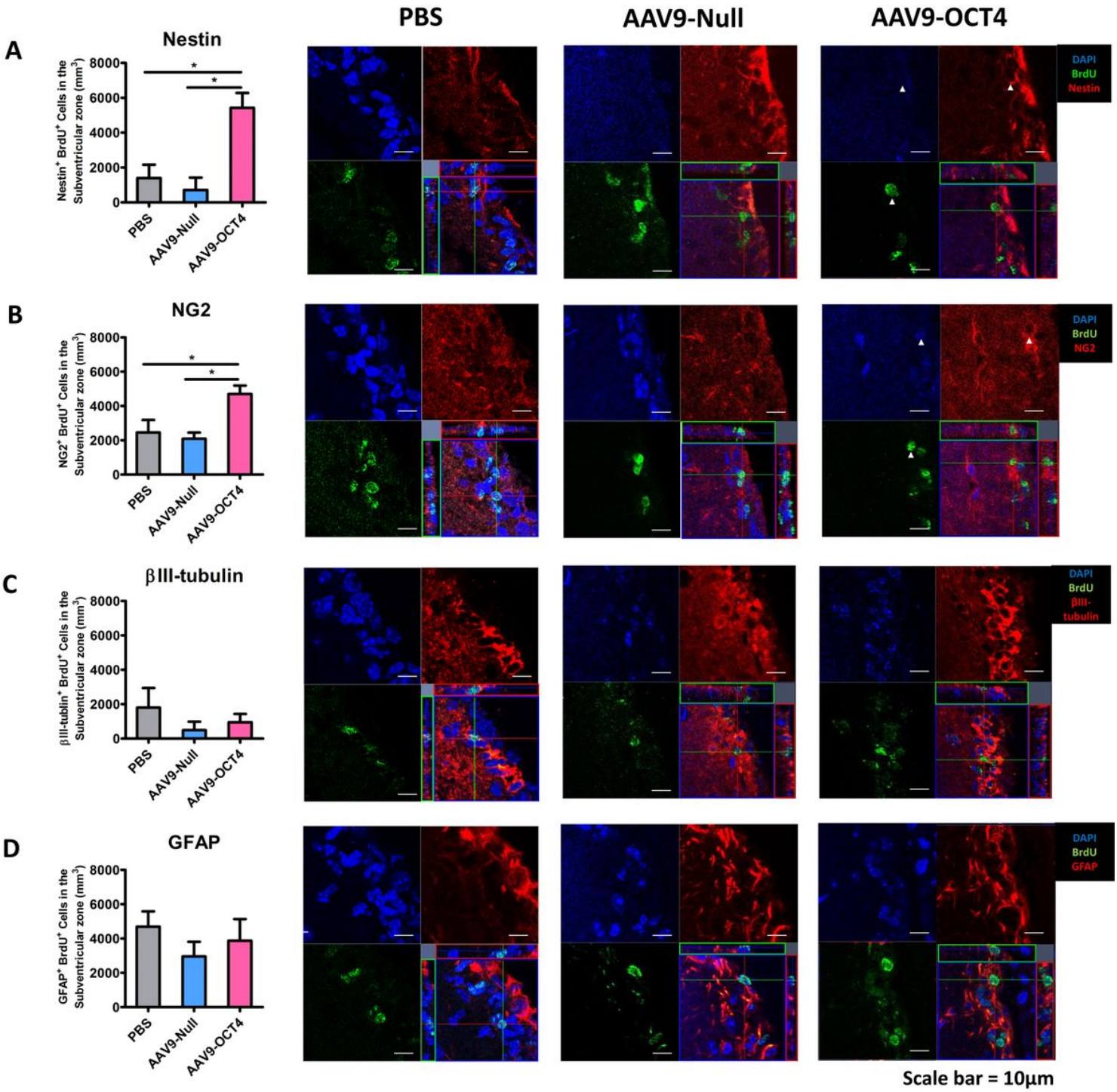

Figure 2

. In situ expression of OCT4 increases oligodendrocyte progenitor cells in the subventricular zone. (A-D) To confirm that OPC-related genes proliferation in the SVZ among three groups 2 weeks after stereotaxic

injection by using confocal microscopy. The numbers of Nestin+BrdU+ (A) and NG2+BrdU+ (B) cells were significantly higher in the AAV9-OCT4 group than control groups. whereas the numbers of βIII-tubulin+BrdU+ (C) and GFAP+BrdU+ (D) cells did not significantly differ among the three groups. *p<0.05, Data in all panels represent mean ± SEM. OCT4: octamer-binding transcription factor 4, AAV9: adeno-associated virus serotype 9, OPC: oligodendrocytes progenitor cell, SVZ: subventricular zone, NG2: neural/glial antigen 2, BrdU: 5-bromo-2'-deoxyuridine, GFAP: glial fibrillary acidic protein

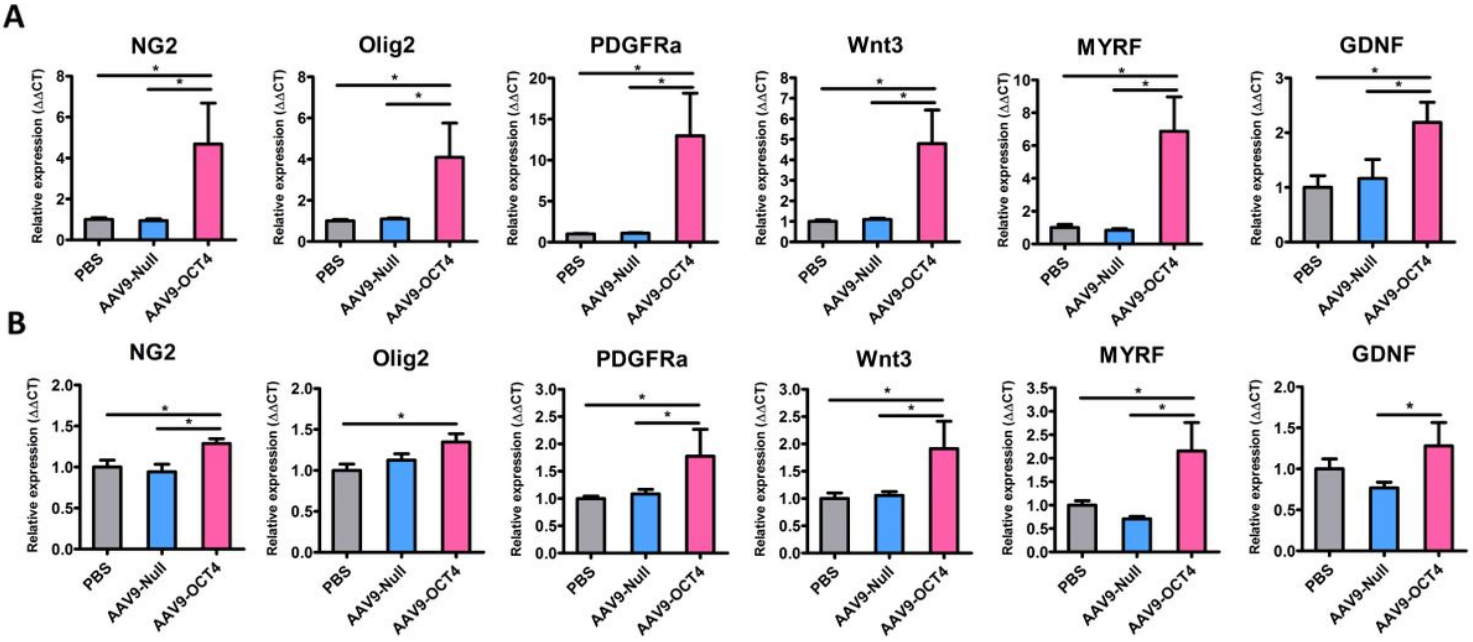

Figure 3

In situ expression of OCT4 increases OPC-related genes. (A,B) To confirm that OPC-related genes proliferation in the cortex (A) and striatum (B) among three groups at 13 weeks of age by using real-time qRT-PCR. AAV9-OCT4 group significantly increased expression levels of NG2, Olig2, PDGFRa, Wnt3, MYRF and GDNF in the cortex and striatum. *p<0.05, Data in all panels represent mean ± SEM. OPC: oligodendrocytes progenitor cell, qRT-PCR: quantitative reverse transcription polymerase chain reaction, OCT4: octamer-binding transcription factor 4, AAV9: adeno-associated virus serotype 9, NG2: neural/glial antigen 2, Olig2: oligodendrocyte transcription factor, PDGFRa: platelet-derived growth factor receptor alpha, Wnt3: Wnt family member 3, MYRF: myelin regulatory factor, GDNF: glial cell-derived neuroprotective factor

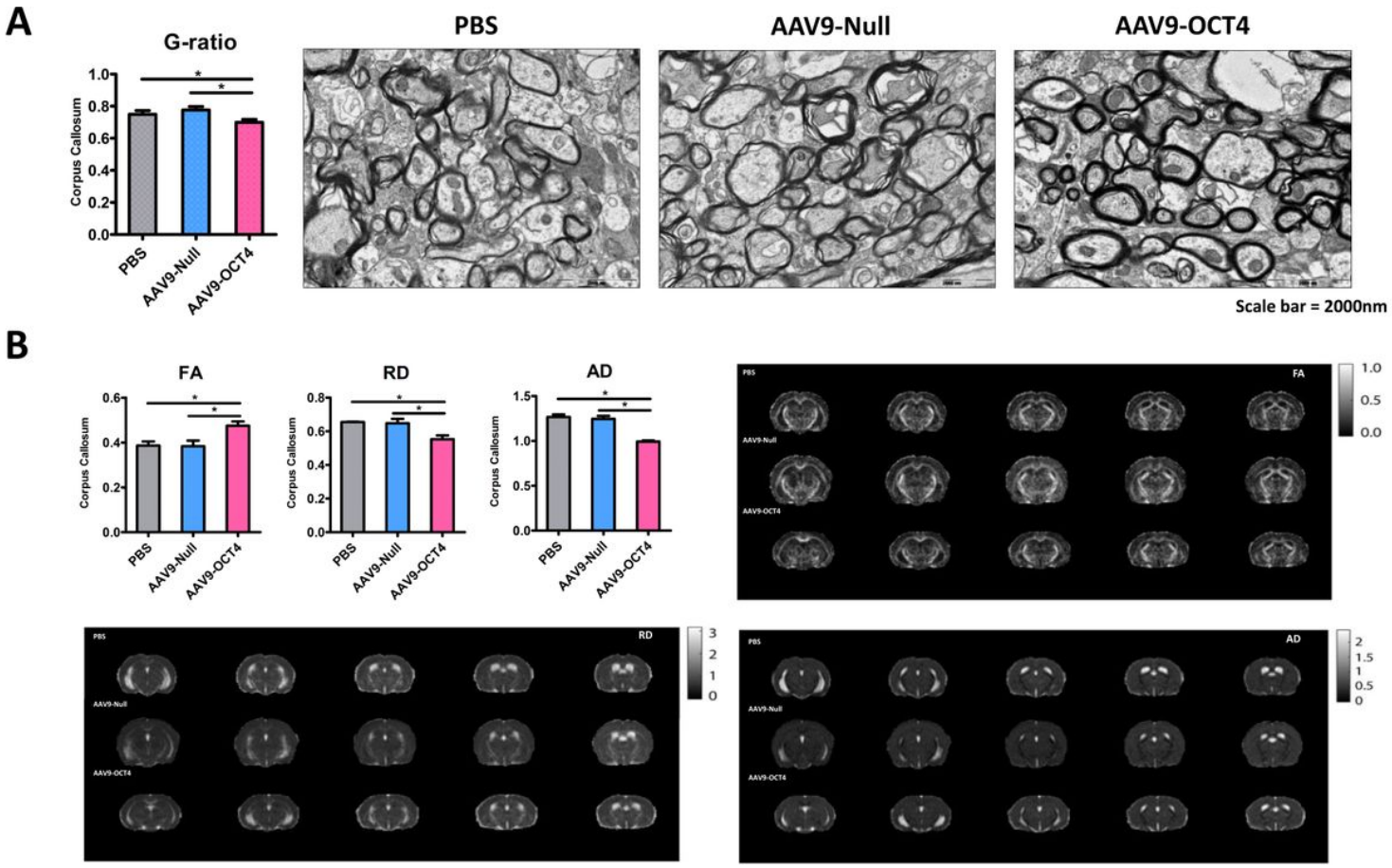

Figure 4

OCT4-induced oligodendrocyte progenitor cells ameliorate myelination deficits (A) Transmission electron microscope was used to visualize myelinated fibers in corpus callosum at 13 weeks of age, the value of g-ratio in the AAV9-OCT4 group was significantly lower than control groups. (B) Magnetic resonance imaging results were analyzed for FA, RD and AD, myelination defects in the AAV9-OCT4 group was significantly ameliorated. *p<0.05, Data in all panels represent mean ± SEM. OCT4: octamer-binding transcription factor 4, AAV9: adeno-associated virus serotype 9, FA: fractional anisotropy, RD: radial diffusivity, AD: axial diffusivity

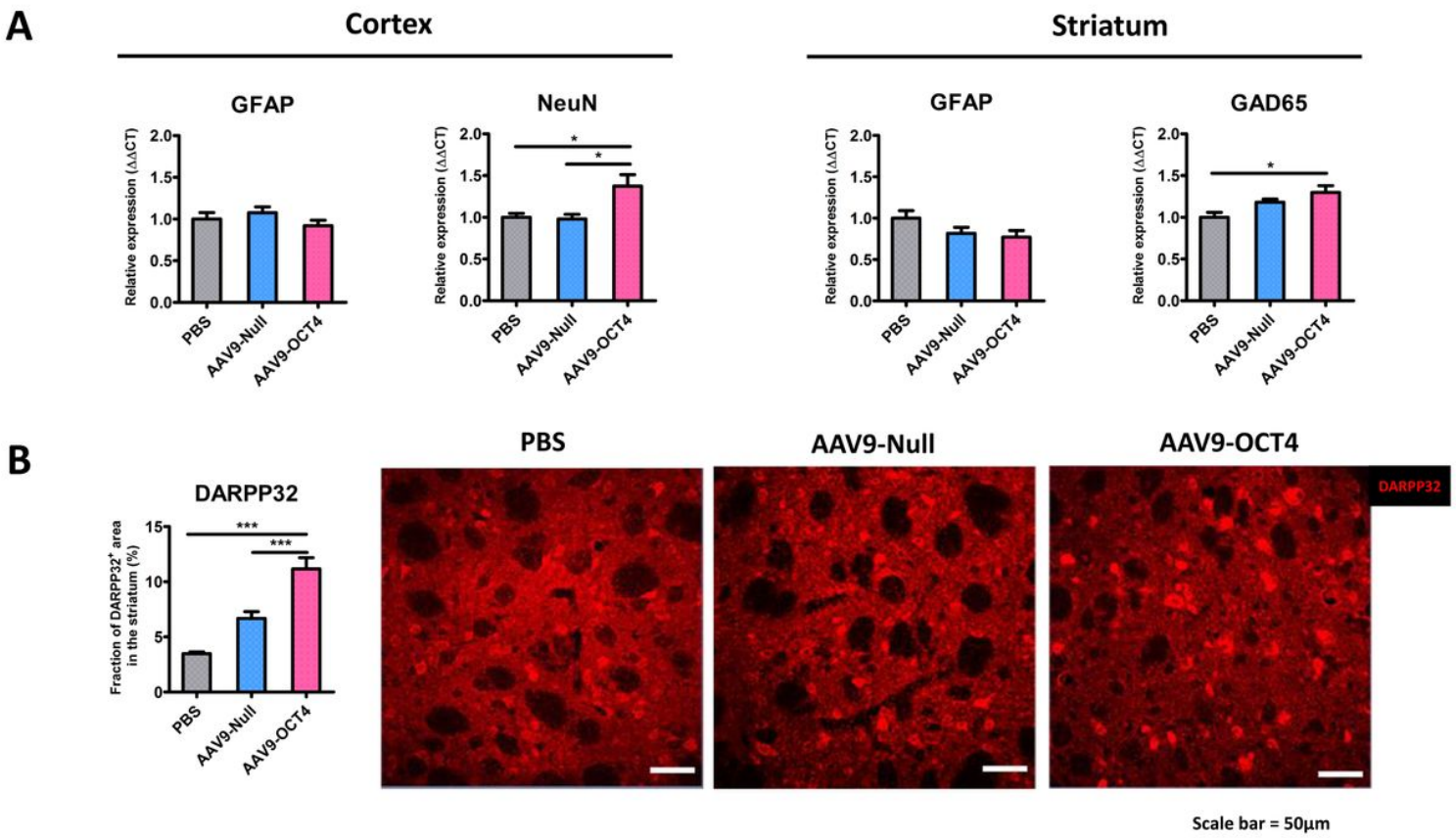

Figure 5

OCT4-induced oligodendrocyte progenitor cells induce neuroprotection. (A) To confirm neuropretection in the cortex (A) and striatum (B) among three groups at 13 weeks of age by qRT-PCR. AAV9-OCT4 group displayed significantly increased expression of NeuN, a mature neuronal marker in the cortex and GAD65, a GABAergic neuronal marker in the striatum. However, the AAV9-OCT4 group did not change the expression of GFAP, an astrocytic marker in both regions (B) In the striatum, AAV9-OCT4 group significantly increased the area of DARPP32+ GABAergic neurons by using confocal microscopy at 13 weeks of age. *p<0.05, ***p<0.001, Data in all panels represent mean ± SEM. OCT4: octamer-binding transcription factor 4, qRT-PCR: quantitative reverse transcription PCR, AAV9: adeno-associated virus serotype 9, NeuN: neuronal nuclei, GAD65: glutamic acid decarboxylase 65, GFAP: glial fibrillary acidic protein, DARPP32: dopamine- and cAMP-regulated neuronal phosphoprotein

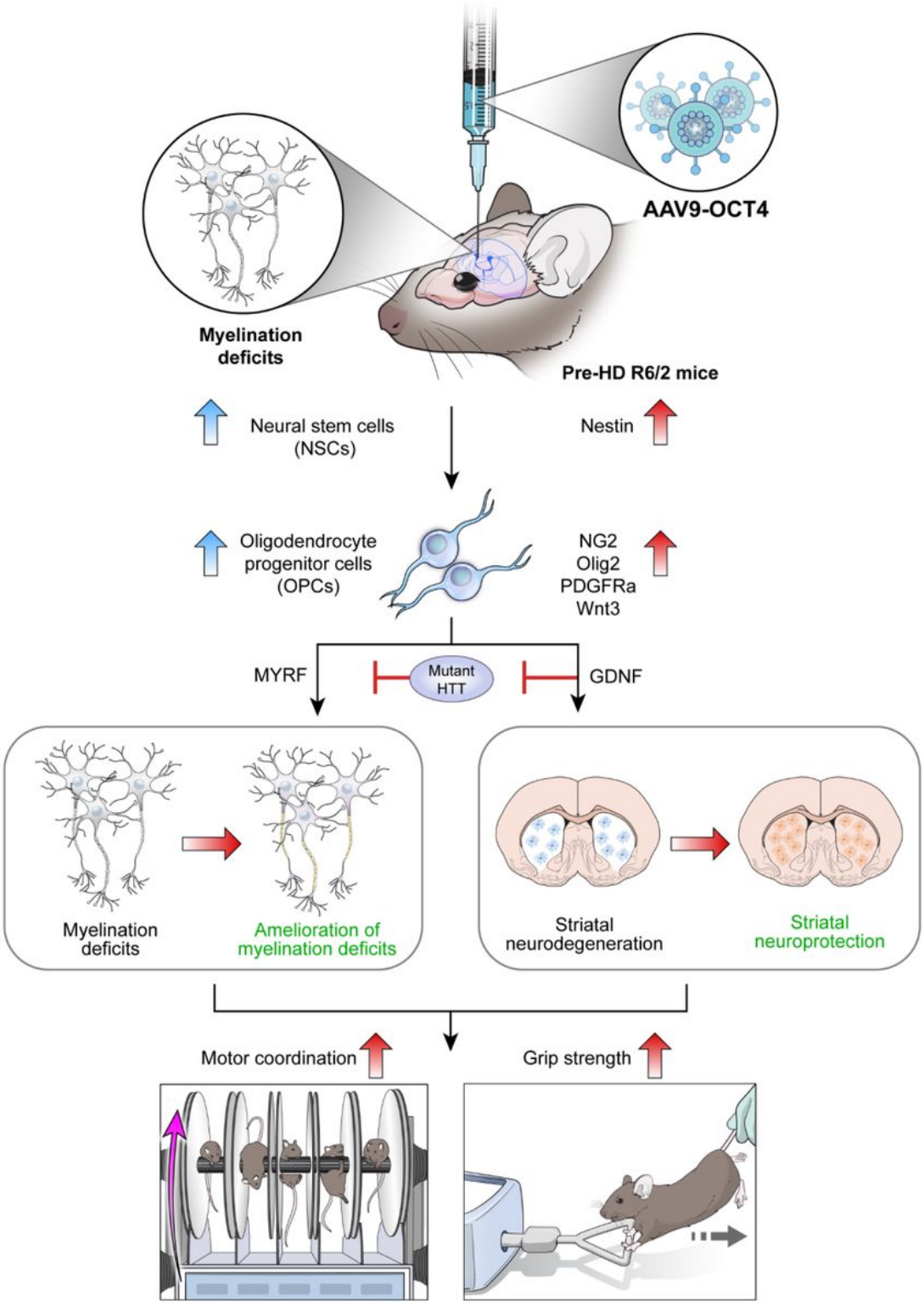

Figure 6

Scheme of in vivo expression of reprogramming factor OCT4 in R6/2 HD mice. Myelin deficits emerge in the corpus callosum at 4 weeks of age, pre-symptomatic (pre-HD) stage before remarkable GABAergic neuronal loss at late-symptomatic (late-HD) stage in R6/2 mice. In situ expression of reprogramming factor OCT4 induces NSC niche activation in the SVZ and changes cell fate specific to the microenvironment of HD from NSCs to OPCs. Particularly, MYRF and GDNF released by OCT4-induced

OPCs seem to ameliorate myelination deficits and induce striatal neuroprotection, consequently improving behavioral performances such as motor coordination and grip strength in HD. OCT4: octamer-binding transcription factor 4, HD: Huntington's disease, SVZ: subventricular zone, NSC: neural stem cell, OPC: oligodendrocytes progenitor cell, MYRF: myelin regulatory factor, GDNF: glial cell-derived neuroprotective factor